Sun Angle, View Angle, and Background Effects on Spectral Response of Simulated Balsam Fir Canopies

K. J. Ranson, C. S. T. Daughtry, and *L. L. Biehl*
Laboratory for Applications of Remote Sensing, Purdue University, West Lafayette, IN 47907

ABSTRACT: An experiment is described that examines the effects of solar zenith angle and background reflectance on the composite scene reflectance of small balsam fir (*Abies balsamea* (L.) Mill.) arranged in different densities. In this study, the shape, density, and, consequently, the needle area index and phytomass of the canopies, as well as the background reflectance, were controlled.

The effects of sun angle, view angle, and background reflectance on the multispectral response of small balsam fir trees were significant. Regression models relating spectral vegetation indices (i.e., normalized difference (ND) and greenness (GR) to phytomass showed very poor relationships ($R^2 = 0.0$) for balsam fir canopies with a grass background. However, strong linear relationships were found for ND ($R^2 = 0.9$) and GR ($R^2 = 0.8$) with phytomass for a background that simulated the reflectance of snow. Changing solar zenith angle significantly affected the models relating ND to phytomass for the snow background, but was not significant in the model relating GR to phytomass for the snow background.

The spectral properties of the background may confound changes in the spectral response of the overstory vegetation. Based on our results, winter-time data, when snow masks the understory, would provide better estimates of overstory phytomass in coniferous forests than would summer-time data.

INTRODUCTION

THE WORLD'S FORESTS are important for storage of carbon and exchange of CO_2 with the atmosphere. Large tracts of forests are being harvested at an alarming rate to provide fuel and fiber and to make room for agricultural development. Some forests downwind from industrial areas are declining, presumably due to acidic precipitation and/or ozone (Lefohn and Brockson, 1984). The effects of large-scale losses in forests on the global ecosystem are unknown at present. It is increasingly important to be able to quantify the present status and potential productivity of global forest resources.

The usefulness of remote sensing data for quantifying the leaf area index (ratio of one-sided green leaf area per unit of ground area) and phytomass has been demonstrated for agricultural canopies (eg., Kollenkark *et al.*, 1982; Asrar *et al.*, 1984). Because leaf area index (LAI) and phytomass are key determinants of net primary production (NPP) in plant canopies, it follows that remote sensing technology may contribute valuable information for understanding the changes in our global ecosystem (Botkin and Pecan, 1982).

The reflectance measured from forest scenes may vary with solar illumination angle, viewing angle, understory or background reflectance, atmospheric effects, as well as intrinsic canopy parameters of phytomass and LAI. Early studies using broad-band solarimeters showed increased reflectance as solar zenith angle increased (Stewart, 1971; Jarvis *et al.*, 1976). Jarvis *et al.* (1976) also noted that the diurnal variation of Sitka spruce (*Picea sitchensis* (Bong.) Corr.) was less than that reported for Scotch pine (*Pinus sylvestris* L.). Greater surface roughness and, thus, greater light-trapping efficiency of the spire-shaped crowns of sitka spruce versus the rounded crowns of Scotch pine was cited as the cause of this difference. Diurnal reflectance studies by Kriebel (1979) and Kimes *et al.* (1980) showed a dependence of the reflectance from coniferous forests on solar zenith angle. Kriebel (1978) reported an increase in reflectance as zenith view angle increased for four vegetated surfaces including a coniferous forest. Overall, data for the bidirectional reflectance of forest canopies is scarce.

The understory or background reflectance can also be important to the composite scene reflectance from forests. In a study of a deciduous forest in northern Minnesota, Badhwar *et al.* (1983) found that the understory reflectance limited their attempts to infer

PHOTOGRAMMETRIC ENGINEERING AND REMOTE SENSING,
Vol. 52, No. 5, May 1986, pp. 649–658.

0099-1112/86/5205-649$02.25/0

TABLE 1. DESCRIPTION OF WAVELENGTH BANDS OF BARNES MODULAR MULTIBAND RADIOMETER (MMR) AND CORRESPONDING LANDSAT THEMATIC MAPPER CHANNELS. MMR BAND 8 WAS NOT USED IN THIS ANALYSIS.

MMR Band	TM Band	Wavelength
		μm
1	1	0.45 - 0.52
2	2	0.52 - 0.60
3	3	0.63 - 0.69
4	4	0.76 - 0.90
5	—	1.15 - 1.30
6	5	1.55 - 1.75
7	7	2.08 - 2.35
8	6	10.60 - 12.50

LAI of aspen (*Populus tremuloides* Michx.).

The success of studies designed to examine the effects of sun angle, view angle, and background reflectance on remote sensing data is often related to the experimenter's ability to obtain detailed measurements of the scene. If the scene could be controlled to a good degree of certainty, those factors of interest could be examined with increased confidence. For this reason an experiment was designed to examine the effects of solar zenith angle and background reflectance on the composite scene reflectance of small balsam fir (*Abies balsamea* (L.) Mill.) arranged in different densities. A linear model relating phytomass to spectral vegetation indices was also evaluated. In this study, the shape, density, and, consequently, the LAI and phytomass of our canopies, as well as the background type, were controlled. All reflectance data were acquired under clear skies and short path length so that atmospheric effects were negligible.

METHODS

A series of four experiments was initiated in the fall of 1983 and continued during the summer of 1984. Seven-year-old balsam fir trees planted in 28-litre pots were purchased from a nursery. Balsam fir has a symmetrical, pyramidal crown and linear-flattened needles and is considered the principal boreal forest fir of North America (Spurr, 1964). The trees were arranged on a 4.0-m diameter rotating platform (turntable) at three densities as described below. Backgrounds of Kentucky bluegrass (*Poa pratensis* L.) sod, and white- and black-painted boards were alternately placed beneath the trees and spectral reflectance was measured.

Three multiband radiometers (Barnes Engineering Company Model 12-1000) were used for spectral measurements. This instrument is sensitive to visible, near-infrared, middle-infrared, and thermal radiation as described in Table 1. The thermal band was not used in our experiment. One radiometer was attached to a boom and leveled to view the scene in the nadir direction. A second radiometer

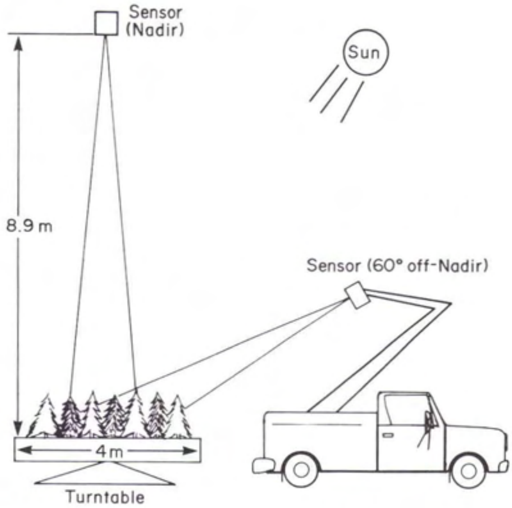

FIG. 1. Arrangement of sensors for balsam fir turntable experiment.

was placed on the boom of an aerial-tower truck and positioned to view the scene at off-nadir angles (Figure 1). The third instrument was mounted on a tripod to view a 1.2 by 1.2-m reference panel painted with barium sulfate. Periodically, this instrument was also used to measure the reflectance of representative samples of the background materials. Estimates of the amount of diffuse irradiance were also obtained by measuring the reflectance of the reference panel shielded from direct sunlight.

With a background in place beneath the trees, radiometric measurements were made for each 10° rotation of the turntable (0 to 360°). Each of the 36 different angles of the turntable presented a slightly different balsam fir canopy to the sensors. A complete rotation of the turntable took about 5 minutes. Changing backgrounds required about 8 minutes. A complete set of 36 observations for all three backgrounds was completed in less than 45 minutes. The maximum change in solar zenith angle was less than 2° for a set of observations for a given background and about 5° for a group of all three backgrounds.

Spectral measurements were collected over the reference panel every 30 seconds and used to convert the voltages measured by the other instruments to reflectance factor (RF). (RF is defined as the ratio of the radiant flux reflected by a sample surface to that which would be reflected into the same reflected-beam geometry by an ideal (lossless) perfectly diffuse (Lambertian) reference surface irradiated in the same way as the sample (Nicodemus *et al.*, 1977)). The reference data were corrected to compensate for the non-Lambertian properties of barium sulfate paint at illumination angles greater than 55°, as noted by Kimes and Kirchner (1982). Correction factors were derived from goniometric measurements of the reference panel made in the laboratory. The three instruments were correlated to each other from simultaneous measurements of the reference panel.

We were unable to measure the spectral reflectance of the small balsam fir trees directly so, for comparison purposes, we estimated the reflectance of sunlit trees using a simple model: i.e.,

$$R_T = (R_C - R_B A_B)/A_T \qquad (1)$$

where R_C is the composite scene RF, R_B is the RF of the background, and A_T and A_B are the proportions of the scene occupied by trees and background, respectively.

Two spectral vegetation indices were utilized in this study. The normalized vegetation index or normalized difference (ND) was calculated as (RF4-RF3)/(RF4+RF3) where RF3 and RF4 are Band 3 (Red) and Band 4 (near-IR) RFs. The Tasseled Cap feature greenness (GR) (Kauth and Thomas, 1976) was calculated from coefficients derived by Crist *et al.* (1984): i.e.,

$$\mathrm{GR} = -0.1603(\mathrm{RF1}) - 0.2819(\mathrm{RF2}) - 0.4934(\mathrm{RF3}) + 0.7940(\mathrm{RF4}) - 0.0002(\mathrm{RF6}) - 0.1446(\mathrm{RF7}) \qquad (2)$$

where RF1, RF2,. . ., RF7 are the RFs in Barnes radiometer bands (Table 1). A constant of 20.0 was added to each calculated GR value to avoid negative values.

In addition to reflectance factor, several measurements of the balsam fir trees were also made. These included height, crown diameter, percent cover, dry phytomass, and needle area index (NAI). Tree heights were measured from the background surface to the top of the leader; crown diameters represent the average of two orthogonal measurements across the base of the crown. Percent cover (A_T in Equation 1 multiplied by 100) was estimated by projecting scene photographs on a dot grid and computing the percentage of dots hitting foliage. Phytomass was estimated by weighing oven-dried (70° for 48 h) needles and branches separately for ten trees. Mean needle area per tree was estimated as the total dry weight of needles multiplied by the needle area to dry weight ratio. The projected areas of 32 samples of 50 needles were determined by planimetering photographs of the needles. The average needle area per tree was multiplied by the density of trees for a given experiment to obtain the needle area index. The measured canopy characteristics for our experiments are listed in Table 2.

Experiment I

The first experiment was conducted on 27 October 1983. The balsam fir trees were placed on the turntable in an equidistant arrangement with a between-tree spacing of 0.76 m. The trees had an average height of 1.05 m, but varied between 0.67 and 1.37 m. Average crown diameter was 0.75 m and percent cover was 74 percent (Table 2). For this experiment, nadir reflectance measurements were acquired with a 15° field of view. Spectral data were limited by the large solar zenith angles that occur at our latitude (40° 30′N) at this time of year (Table 3).

Experiment II

A second experiment was conducted on 25 June 1984. Newly acquired balsam fir trees were placed on the turntable with a spacing of 0.61 m, resulting in a percent cover of 91 percent (Figure 2a). The trees were pruned to a uniform height of 1.05 m.

In addition to the nadir zenith view angle used in Experiment I, spectral data were also acquired at a 60° view zenith angle and with view azimuth angles within 30° of the sun's principal place for both forward- and backscattering directions. The addition of the off-nadir view zenith angle required a decrease in the angular FOV of the radiometers to 10°.

Experiment III

On 19 July 1984, the turntable was populated with trees at a spacing of 0.76 m, as in Experiment I. Dot grid estimates of average percent cover were 70 percent (Figure 2b). Spectral data were acquired from mid-morning to early afternoon with the same procedures used in Experiment II.

Experiment IV

A final experiment was performed on 18 September 1984 with trees arranged on the turntable with a spacing of 0.91 m and 52 percent cover (Figure 2c). At this rather wide spacing of the trees, a noticeable row effect was present, especially at larger solar zenith angles and with the white background. The equidistant arrangement of the trees resulted in a large amount of sunlit background whenever a row of trees lined up with the sun. This resulted in higher reflectances at 60° intervals of turntable rotation. To minimize this "row" effect, these data points were deleted. This effect was most noticeable for the highly reflecting white background. However, to compare background effects, we imposed this constraint on measurements with grass and black backgrounds for the low-density canopy as well. The overall effect was reduced mean reflectance and decreased variation. A similar effect was present in our data for off-nadir reflectance measurements. Thus, we also deleted those data values acquired when the sensor was looking directly down a row. Table 3 summarizes the spectral data collected over the course of the four experiments.

RESULTS AND DISCUSSION

Background Reflectance

The balsam fir canopies, as arranged on the turntable and viewed by a sensor, consisted of a mixture of trees and background. The amount of each com-

TABLE 2. MEAN BALSAM FIR CANOPY CHARACTERISTICS FOR FOUR EXPERIMENTS. STANDARD DEVIATIONS ARE SHOWN IN PARENTHESIS.

Experiment	Date	Spacing	Height	Crown Diameter	Phytomass	Needle Area Index	Canopy Cover
		m	m	m	kg/m²		%
I	27 Oct 1983	0.76	1.04 (0.13)	0.73 (0.10)	1.50 (0.38)	3.5 (0.9)	74 (3)
II	25 Jun 1984	0.61	1.05 (0.04)	0.72 (0.12)	3.04 (0.49)	7.4 (0.9)	91 (1)
III	17 Jul 1984	0.76	1.05 (0.04)	0.72 (0.12)	1.95 (0.31)	4.8 (0.6)	70 (4)
IV	19 Sep 1984	0.91	1.05 (0.04)	0.72 (0.12)	1.35 (0.22)	3.3 (0.4)	52 (3)

TABLE 3. SOLAR ANGLES AND NUMBER OF REFLECTANCE DATA SETS FOR BALSAM FIR CANOPIES.

Experiment	Date	Sun Angle Range: Zenith	Sun Angle Range: Azimuth	No. of Sets*: G	No. of Sets*: W	No. of Sets*: B	Zenith View Angles
		degrees	degrees				degrees
I	27 Oct 1983	57–76	205–239	3	3	3	0
II	25 Jun 1984	17–65	113–280	9	8	8	0,60
III	17 Jul 1984	20–34	115–209	4	4	4	0,60
IV	19 Sep 1984	39–79	150–263	7	7	7	0,60

*G = Trees with grass background
W = Trees with white background
B = Trees with black background

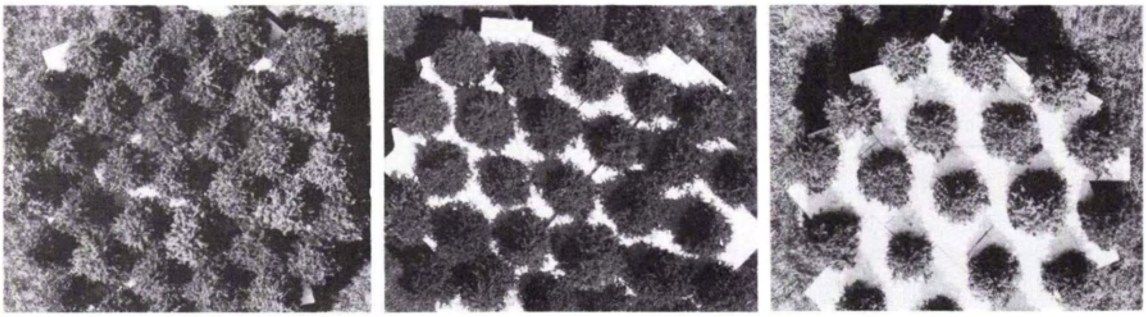

(a) (b) (c)

FIG. 2. Vertical photographs of high (a), medium (b), and low density (c) balsam fir canopies arranged on the turntable with a white background.

ponent in the FOV depends on the arrangement of the trees and the angle of view. The composite scene reflectance depends on the amount of each component in the scene and their respective spectral reflectances. RFs for the three backgrounds are shown in Figure 3. For comparison, the spectral reflectance factors for sunlit balsam fir estimated with Equation 1 are also shown. The data used to estimate the example reflectance curve for the balsam fir canopy were acquired from the high density canopy under a solar zenith angle of 18°, so shadows cast by the trees upon the background were negligible. RFs of balsam fir estimated with Equation 1 were similar to the RF of grass background in the visible and near IR wavebands, but differed in the middle IR, with grass having higher RFs (Figure 3). The balsam fir RFs were also quite similar to those for the black background in Band 1 (0.42 to 0.52 μm), Band 3 (0.63 to 0.69 μm), and Band 7 (2.08 to 2.35 μm).

The background RFs changed slightly with illumination angle. Normalized difference (ND) and greenness (GR) for the three backgrounds measured

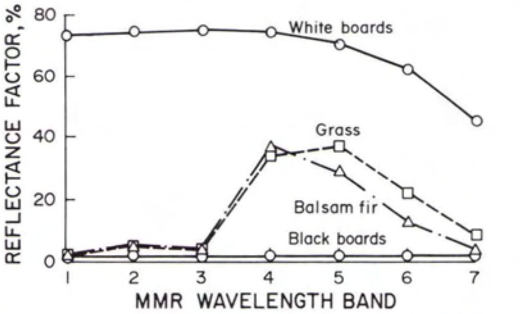

FIG. 3. Reflectance factors (RF) of grass, white, and black backgrounds in MMR wavebands. Estimated RF of balsam fir tree is also shown. Solar zenith angle during measurements was about 18°.

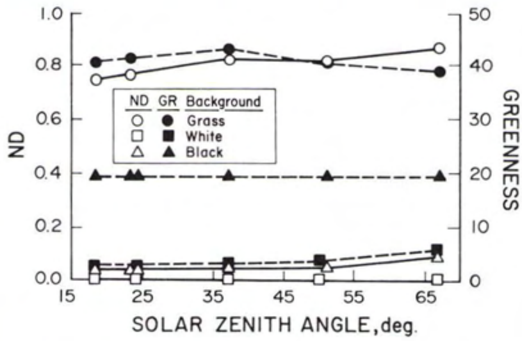

FIG. 4. Changes in normalized difference (ND) and greenness (GR) of grass, white, and black backgrounds as a function solar zenith angle.

at varying solar zenith angles are shown in Figure 4. For ND, a general increase in response with solar zenith angle was apparent for the grass and black backgrounds while the white background response remained essentially zero. GR for black background response was constant through the day, but GR for white background increased slightly at solar zenith angles greater than 50°. The initial slight increase and then decrease in both GR and ND for grass was probably related to the condition of the grass sod and not to extrinsic factors such as varying irradiance. Examination of calibration panel data and total incidence pyranometer data revealed no significant changes in irradiance that would account for the observed variation.

COMPOSITE SCENE REFLECTANCE

Figure 5 illustrates the behavior of ND to changes in solar zenith angle for nadir and 60° view zenith in the forward and backscatter directions for low and high density canopies (Experiments IV and II, respectively) for the three backgrounds. The behavior of ND for the medium density canopies was intermediate and was omitted for clarity. With grass background, ND values were high (> 0.8) for both canopies and all illumination and view angles. The nadir-viewed ND increased as solar zenith angle increased for both canopies and all backgrounds. ND measured at 60° view zenith in the forward-scattered direction did not vary significantly with solar zenith angle for most cases. The exception was the black background where ND decreased between 65° and 79°. ND in the backscatter direction tended to increase for the low density canopy (Figures 5a, c, and e) and decreased for the high density canopy (Figures 5b, d, and f).

Greenness (GR) responded differently than ND to changes in background, solar zenith angle, and viewing angle (Figure 6). Nadir GR decreased as solar zenith angle increased for both canopies with grass and for the high density canopy with white and black backgrounds (Figures 6a, b, d, and f). For the low density canopy with white and black backgrounds, nadir GR showed a slight linear increase as solar zenith angle increases (Figure 6c and e). Significant increased in GR were observed for both backscattered and forward-scattered directions for the 60° view zenith angle for most cases. The exceptions were the low-density white and black backgrounds where GR in the backscattered direction did not vary significantly with sun angle because of the large variances of the measurements (Figures 6c and e).

The data presented above indicate the complexity of interpreting spectral response from heterogeneous scenes. However, if the spectral response of the scene is considered as a composite effect of vegetation and background, each with sunlit and shaded components, the nature of the trends becomes apparent.

The light-scattering behavior of green vegetation is strongly wavelength dependent (Knipling, 1967). Green, chlorophyll-containing leaves strongly absorb red sunlight and reflect and transmit a large proportion in the near-IR. Thus, homogeneous canopies with large amounts of green leaves are highly reflective in the near-IR, but reflect very little in the red region. The ND for a homogeneous dense canopy will approach a value of 1.0. For heterogeneous scenes, the effects of background reflectance and shadows cast by the trees must also be considered.

For example, consider the trends of ND with solar zenith angle for nadir measurements. The observed NDs for both high and low density canopies (Figures 5a and b) were only slightly greater than ND of the grass background alone (Figure 4). This is because of the similar red and near-IR reflectance of trees and grass (Figure 3) in our experiments. The increase in ND as solar zenith angle increased occurred because of the differential scattering of red and near-IR radiance by the canopy and background. When the sun was higher above the horizon (small solar zenith angle), the nadir-viewing sensor received more

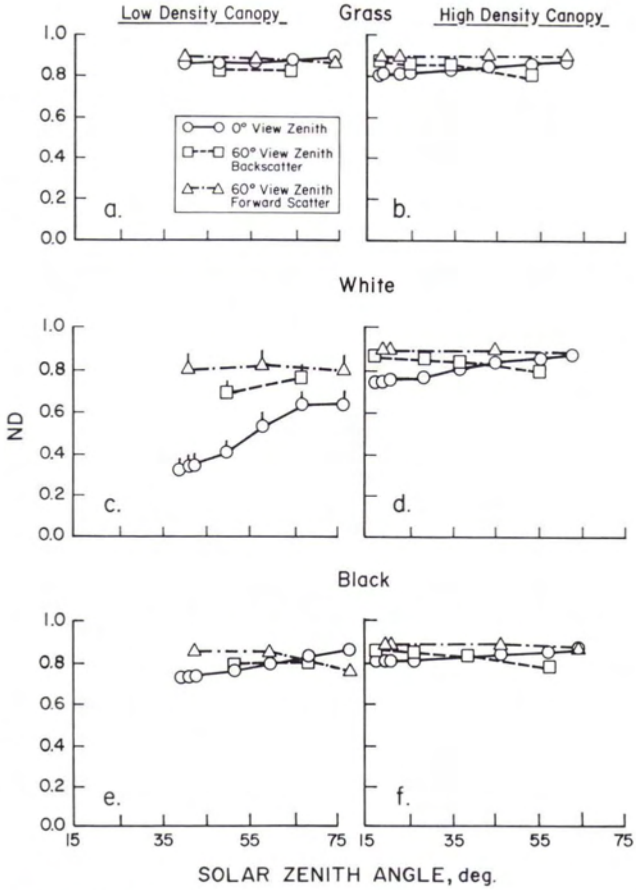

FIG. 5. Mean normalized difference (ND) variation with solar zenith angle for low and high density balsam fir canopies with different back grounds and sensor viewing geometries. Vertical bars indicate one standard deviation. For data points without vertical bars, standard deviations were less than or equal to symbol height.

reflected light from directly illuminated areas of the scene. As the solar zenith angle increased, the probability of tree foliage intercepting solar irradiance also increased. Because near-IR transmittance by green leaves is an order of magnitude greater than that of the red band, red reflectance decreases at a higher rate than near-IR. Thus, the shaded portions of the scene could be expected to have higher ND values than directly illuminated areas.

The trends for the highly reflecting white background dramatized the effects of shadows on ND (Figures 5c and d). At the highest sun positions (i.e, smallest zenith angles), contributions of directly illuminated background to the scene reflectance were greatest and ND values were at the observed minimum for both high and low canopies. As sun zenith angles and shadows increased, the proportion of directly illuminated background decreased and the contribution of the background to scene reflectance also decreased. However, the absolute difference between red and near-IR RFs increased, and ND increased. This was especially evident for the low density canopy with white background (Figure 5c) where ND increased from 0.3 at a sun angle of 35° to over 0.6 at a solar zenith angle of 65°. These results are consistent with the greater sun-angle dependence of reflectance from agricultural canopies with row structure reported by Pinter *et al.* (1983) and Ranson (1983).

The generally high values of ND for off-nadir measurements were a result of the sensor viewing more canopy and less background. When the view direction is toward the sun (forward-scattering), a large proportion of the scene is shaded and ND is high. Note that when the solar zenith angle was very large (e.g., > 75°) ND decreased (Figures 5a, c, and e). The probable cause of this was an increase in the proportion of red band irradiance in the spectral distribution of skylight at very large solar zenith angles.

In the back-scattered direction, the proportion of shadows is reduced and the sensor viewed primarily

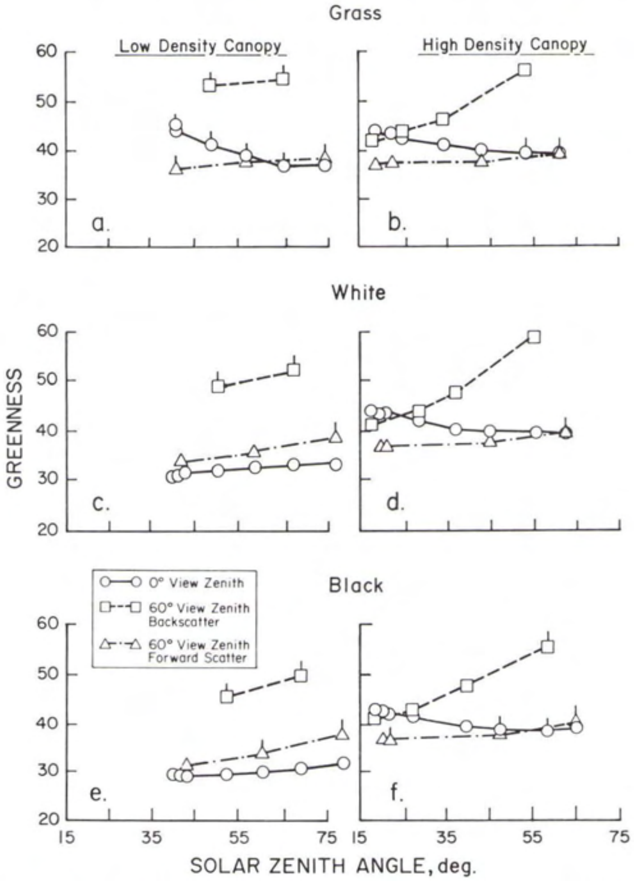

FIG. 6. Mean greenness variation with solar zenith angle for low and high density balsam fir canopies with different backgrounds and sensor viewing geometries. Vertical bars indicate one standard deviation. For data points without vertical bars, standard deviations were less than or equal to symbol height.

directly illuminated needles, branches, and background. This caused the ND response to decrease, as shown in Figures 5b, d, and f. Also, it is possible that at solar zenith angles greater than the "hot spot" angle (i.e., for our data, solar zenith = view zenith = 60°) ND may increase because of increased shadows in the scene. This may explain the increase shown in Figures 5c and e. However, there are insufficient data to directly support this statement.

The effect of increasing solar zenith angle on the greenness (GR) transformation also appeared to be dependent on shadowing. As the sun angle increased, the increased shadows caused an overall darkening of the scene. Because GR is a function of the magnitude of the reflectance and not relative differences as in ND, there was an overall decrease of GR with increasing sun angle for the nadir view (Figures 6a, b, d, and e). This also explains the low GR values measured for the forward-scatter direction. The increase in GR noted for the low density canopy with white and black backgrounds was caused by a nearly constant decrease in RFs for all bands as sun angle increased (Figures 6c and e).

Viewing the canopies in the back-scattered direction resulted in increased GR as sun angle increased. This is related to the increased amount of directly illuminated scene components as the solar zenith angle approached the hot spot.

Our results demonstrate that careful consideration of sun angle, view angle, and background characteristics is necessary to understand the spectral reflectance from heterogeneous scenes such as forests. However, of keen interest to resource managers is understanding how to interpret multispectral data and to infer specific attributes of the forest canopy. For example, the relationships of normalized difference and greenness to green LAI and phytomass of agricultural crops are well known (Tucker, 1979; Kollenkark *et al.*, 1982; Pinter *et al.*, 1983). Tucker *et al.* (1985) have even related ND to phytomass over the entire African continent.

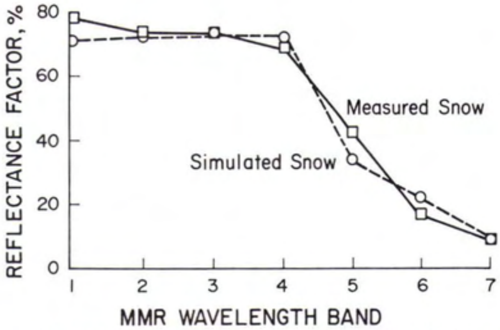

FIG. 7. Comparison of spectra for snow-covered lake and simulated snow derived by combining spectral reflectance measurements for white and grass backgrounds. Snow spectra provided by G. Badhwar, NASA Johnson Space Center, Houston, Texas.

RELATIONSHIP OF SPECTRAL VARIABLES TO CANOPY PHYTOMASS

In order to examine some relationships of spectral response to phytomass for balsam fir, the nadir-measured data for all four experiments were combined. To evaluate these relationships for conditions that approximate balsam fir and natural backgrounds, we analyzed composite scene reflectance data from the grass background. In addition, we also created a new data set for the balsam fir canopy reflectance with a background that approximated the spectral characteristics of freshly fallen snow. Published values of the nadir reflectance of snow (Dirmhirn *et al.*, 1979; Obrien and Munis, 1975) indicate that the reflectance factors for fresh snow are high in the visible and near-IR (> 70 percent), but low (< 20 percent) in the middle-IR regions. None of the three backgrounds individually approximated the spectra of snow. However, using the visible and near-IR RFs from the white background with middle-IR RFs measured from the grass background provided spectra that approximate snow. Figure 7 presents an example of simulated snow background RFs compared with data measured over a snow-covered lake on 3 December 1983 in northern Minnesota (G. Badhwar, personal communication). Because composite scene reflectance data for the balsam fir canopies were acquired from grass and white background scenes under similar solar zenith angles, we combined visible and near-IR RF data from canopies with white background with middle-IR RF data from canopies with the grass background to create a new data set to simulate the spectral response of canopies with a snow background. With this procedure, ND values for canopies over simulated snow will be the same as those for the white background. GR values, however, will be slightly higher than for the white background because of lower middle-IR RFs and the negative coefficients for these bands (see Equation 2). Freshly fallen snow has nearly Lambertian reflectance characteristics (Suits, 1978) although Knowles Middleton and Mungall (1952) suggest that this is true only for zenith angles of incidence less than 45°. For our purposes, we will assume that spectral reflectance of the simulated snow background is a reasonable approximation of freshly fallen snow.

Multiple linear regression analysis was employed to examine the effect of the backgrounds on the spectral response. The solar zenith angle (θ_s)is included in the model to account for the dependence observed in Figures 5 and 6. The model used was

$$Y = b_o + b_1 X + b_2 \theta_s \tag{3}$$

where Y is the estimated spectral response of either ND or GR, X is phytomass, and b_o, b_1, and b_2 are the multiple regression coefficients. Reflectance factors measured from the backgrounds alone (Figure 4 and Figure 7) were used to represent cases of no balsam fir phytomass.

For the grass background the relationship between the spectral variables and phytomass was very poor; i.e., $R^2 = 0.36$ (Table 4). Regression coefficients for phytomass (b_1) were not significant ($\alpha = 0.20$), as shown in Table 4. Figures 8a and c graphically illustrate these results, that is, the spectrally similar background masks changes due to the density of the trees. Badhwar *et al.* (1984) described a similar effect for an aspen forest.

The high contrast between trees and "snow" background improved the relationships between phytomass and the spectral variables. Regression coefficients for phytomass (b_1) were both highly significant ($\alpha = 0.01$). R^2 values were also greater than 0.80 in both cases (Table 4). The effects of solar zenith angle on ND were significant for phytomass (Table 4). However, for GR the regression coefficients related to solar zenith angle (b_2) were not significantly different from zero ($\alpha = 0.20$) (Figures 8b and d).

Figure 9 presents the relationships of nadir ND and phytomass for data restricted to solar zenith angles between 35 and 45°. The relationship obtained for the grass background was extremely poor ($r^2 = 0.0$) with ND constant over the range of phytomass. On the other hand, the relationship for the "snow" background is strongly linear ($r^2 = 0.99$).

These results demonstrate the potential for estimating forest canopy variables from remote sensing data. Very little information can be extracted when the background spectral response is similar to the overstory. However, when there is higher contrast between the overstory and the understory, both ND and GR may perform well.

CONCLUSIONS

The effects of sun angle, view angle, and background type on the multispectral response of small balsam fir trees are significant. Observed increases

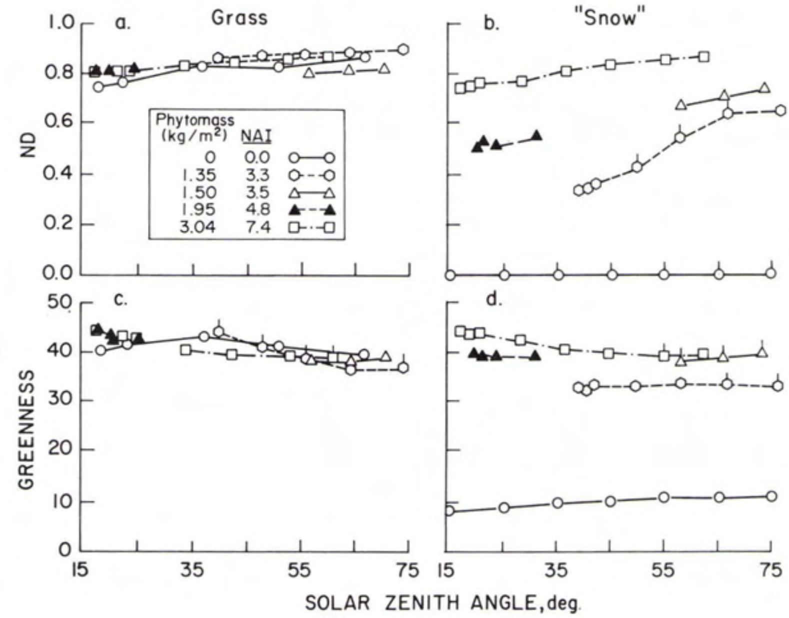

FIG. 8. Changes in normalized difference (ND) and greenness (GR) as a function of solar zenith angle for five densities of balsam fir trees with grass and "snow" backgrounds.

TABLE 4. MULTIPLE REGRESSION COEFFICIENTS FOR RELATIONSHIPS OF NORMALIZED DIFFERENCE (ND) AND GREENNESS (GR) TO PHYTOMASS (X) AND SOLAR ZENITH ANGLE (θ_S). MODEL USED WAS $Y = b_0 + b_1X + b_2\theta_S$.

Background	Spectral Variable	b_0	b_1	b_2	R^2	SE_1	SE_2
Grass	ND	0.78**	0.007	0.001**	0.36	0.005	0.0003
	GR	45.97**	−0.544**	−0.087**	0.28	0.406	0.024
"Snow"	ND	−0.15**	0.274**	0.005**	0.92	0.015	0.001
	GR	10.62**	10.790**	0.074	0.82	0.957	0.055

**Coefficient significant at $\alpha = 0.01$.

in nadir measurements of ND as solar zenith angle increased appear to be caused by the proportionately higher near-IR component within the shadows cast by the trees. This effect was also observed for off-nadir measurements. The effect of the increased red irradiance component present in skylight at very large sun zenith angles may also be important. Care must be taken when interpreting ND data when sun and view angles vary.

The spectral properties of the background may confound changes in the spectral response of the overstory vegetation. Based on our results, wintertime data, when snow masks the understory, would provide better estimates of overstory phytomass in coniferous forests then summer-time data. When extending these principles to actual forests, care must be taken to avoid situations when snow is on the trees.

Obviously, the controlled nature of this study may not totally describe the situation encountered in a natural forest. However, the basic principles of the spectral response from small balsam fir with respect to solar zenith angle, view zenith angle, and background reflectance should provide insight for studies of the natural forest environment.

Experiments such as the one described here can provide significant useful information for understanding the factors that affect the spectral response from forest scenes. In addition, controlled experiments can provide data that may serve as "test beds" for canopy modeling studies. In the future we plan to increase the range of viewing angles in our experiments and also extend our analysis to microwave sensors.

ACKNOWLEDGMENTS

This work was supported by NASA Contract NAS9-

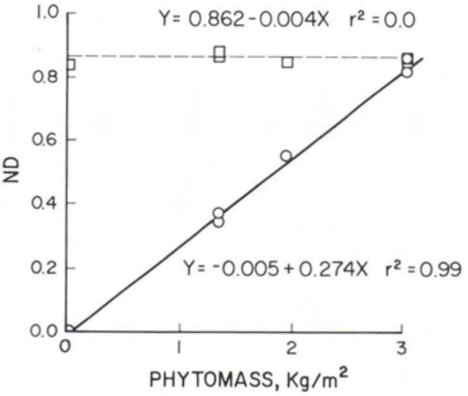

FIG. 9. Relationship of nadir normalized difference (ND) and phytomass for balsam fir canopies with grass (squares) and simulated snow (circles) backgrounds. Data were acquired with solar zenith angles between 35° and 45°.

16528 under the Characterization of Vegetation With Remote Sensors (COVER) project. The authors appreciate the field assistance provided by D. Locks, D. Lindman, and P. Mercer. We gratefully acknowledge the capable assistance of Mary Rice for typing the manuscript.

REFERENCES

Asrar, G., M. Fuchs, E. T. Kanemasu, and J. L. Hatfield, 1984. Estimating absorbed photosynthetic radiation and leaf area index from spectral reflectance of wheat. *Agron. J.* 76:300–306.

Badhwar, G. D., R. B. MacDonald, and F. G. Hall, 1984. Spectral characterization of biophysical characteristics in a boreal forest: Relationship between Thematic Mapper band reflectance and leaf area index for aspen. *IGARSS'84* I:111–115, Strasbourg, France, 27–30 August.

Botkin, D. B., and E. V. Pecan, 1982. *Habitability of the earth: Land-air interactions, world food production, and net primary production*. Report prepared for National Aeronautics and Space Administration from conf. at Univ. of Calif., Santa Barbara, May 1982. 39 p.

Crist, E. P., R. Laurin, J. E. Colwell, and R. J. Kauth, 1984. *Investigations of vegetation and soils information contained in Landsat thematic mapper and multispectral scanner data*. ERIM Tech. Rep. 160300-10-F, Ann Arbor, Michigan.

Dirmhirn, I., and F. D. Eaton, 1979. Reflected irradiance indicatrices of natural surfaces and their effect on albedo. *Appl. Optics* 18:994–1008.

Jarvis, P. G., G. B. James, and J. J. Landsberg, 1976. Coniferous forest, in J. L. Monteith (ed.), *Vegetation and the Atmosphere*, Vol. 2 Case studies. Academic Press, New York, N.Y.

Kauth, R. J., and G. S. Thomas, 1976. The tasseled cap — graphic description of spectral temporal development of agricultural crops as seen by Landsat. *Proc. Symp. Machine Processing Remotely Sensed Data*, LARS/Purdue Univ., W. Lafayette, Indiana, 47906-1399, June 29-July 1. Pp. 4B/41–51.

Kimes, D. S., and J. A. Kirchner, 1982. Irradiance measurement errors due to the assumption of a Lambertian reference panel. *Remote Sens. Environ.* 12:141–149.

Kimes, D. S., J. A. Smith, and K. J. Ranson, 1980. Vegetation reflectance measurements as a function of solar zenith angle. *Photogrammetric Engineering and Remote Sensing* 46:1563–1573.

Knipling, E. B., 1967. Physical and physiological basis for differences in reflectance of healthy and diseased plants, in *Workshop on infra-red color photography in the plant sciences*, Florida Dept. Agric. Winter Haven, Fla. March 2–3.

Knowles Middleton, W. E., and A. G. Mungall, 1952. The luminous directional reflectance of snow. *J. Opt. Soc. Am.* 42:572–579.

Kollenkark, J. C., C. S. T. Daughtry, M. E. Bauer, and T. L. Housley, 1982. Effects of cultural practices on agronomic and reflectance characteristics of soybean canopies. *Agron. J.* 74:751–758.

Kriebel, K. T., 1978. Measured spectral bidirectional reflection properties of four vegetated surfaces. *Applied Optics* 17:253–260.

———, 1979. Albedo of vegetated surfaces: Its variability with differing irradiances. *Remote Sens. Environ.* 8:283–290.

Lefohn, A. S., and R. W. Brockson, 1984. Acid rain effects research - a status report. *J. Air Pollution Control Assoc.* 34:1005–1013.

Nicodemus, F. E., J. C. Richmond, J. J. Hsia, I. W. Ginsberg, and T. Limperis, 1977. *Geometrical considerations and nomenclature for reflectance*. NBS Monograph 160. U. S. Dept. of Commerce, Washington, D. C., 52 p.

Obrien, H. W., and R. H. Munis, 1975. Red and near-infrared spectral reflectance of snow, in A. Rango (ed.), *Operational Applications of Satellite Snowcover Operations*. Workshop Proc., NASA Special Publication SP-391, Washington, DC.

Pinter, P. J., R. D. Jackson, S. B. Idso, and R. J. Reginato, 1983. Diurnal patterns of wheat spectral reflectances. *IEEE Trans. Geosci. Remote Sens.* GE-21:156–163.

Ranson, K. J., 1983. *Angular reflectance characteristics of corn and soybean canopies*. Ph. D. Thesis, Purdue Univ., Univ. Microfilms, (Diss. Abstr. 84-07598), Ann Arbor, Mich., 168 p.

Spurr, S. H., 1964. *Forest Ecology*. Roland Press, New York, N.Y.

Stewart, J. B., 1971. The albedo of pine forest. *Quart. J. R. Met. Soc.* 97:561–564.

Suits, G. H., 1978. Natural sources, in W. L. Wolfe and G. J. Zissis (ed.), *The Infrared Handbook*. Office of Naval Research, Dept of the Navy, Washington, D. C.

Tucker, C. J., 1979. Red and photographic infrared linear combinations for monitoring vegetation. *Remote Sens. Environ.* 8:127–150.

Tucker, C. J., J. G. R. Townshend, and T. E. Goff, 1985. African land-cover classification using satellite data. *Science* 227:369–375.

(Received 29 August 1985; accepted 22 October 1985; revised 13 December 1985)